Gait Transitions for Quasi-Static Hexapedal Locomotion on Level Ground

G. C. Haynes, F. R. Cohen, and D. E. Koditschek

Abstract As robot bodies become more capable, the motivation grows to better coordinate them—whether multiple limbs attached to a body or multiple bodies assigned to a task. This paper introduces a new formalism for coordination of periodic tasks, with specific application to gait transitions for legged platforms. Specifically, we make modest use of classical group theory to replace combinatorial search and optimization with a computationally simpler and conceptually more straightforward appeal to elementary algebra.

We decompose the space of all periodic legged gaits into a cellular complex indexed using "Young Tableaux", making transparent the proximity to steady state orbits and the neighborhood structure. We encounter the simple task of transitioning between these gaits while locomoting over level ground. Toward that end, we arrange a family of dynamical reference generators over the "Gait Complex" and construct automated coordination controllers to force the legged system to converge to a specified cell's gait, while assessing the relative static stability of gaits by approximating their stability margin via transit through a "Stance Complex". To integrate these two different constructs—the Gait Complex describing possible gaits, the Stance Complex defining safe locomotion—we utilize our compositional lexicon to plan switching policies for a hybrid control approach. Results include automated gait transitions for a variety of useful gaits, shown via tests on a hexapedal robot.

G. C. Haynes and D. E. Koditschek
Electrical & Systems Engineering, University of Pennsylvania
200 S. 33rd St, Philadelphia, PA 19104
e-mail: {gchaynes,kod}@seas.upenn.edu

F. R. Cohen
Mathematics Department, University of Rochester
RC Box 270138, Rochester, NY 14627
e-mail: cohf@math.rochester.edu

1 Introduction

Gait transitions are ubiquitous among legged animals and essential for robots. Whereas there is a long and still lively debate about the reason for their value to animal runners (optimized joint loads? [4]; optimized energetics? [5]; muscle function or bone strain? [21]), the more limited capabilities of legged robots ensure for years to come that different maneuvers in different environments at different speeds under varied loading conditions will require the adoption of distinct locomotion patterns, along with necessitating the ability to transition between them safely and efficiently. The great variety of gaits found in nature—quadrupedal walking, trotting, pacing, and galloping; hexapedal wave gaits and alternating tripods [15, 11, 22]; and so on—persuades us of the importance in building a general framework to identify and produce reliable transitions amongst all gaits a robot can use.

A variety of methods have been proposed for switching gaits in legged robots, however most have not considered underactuated systems, in which legs do not have full control over the timing of stance and recirculation throughout a full stride. Examples of underactuated legged robots include the RHex robotic hexapod [17] and the RiSE climbing robot [19], legged machines respectively capable of running and climbing on many unstructured terrains. In the case of RHex, each leg contains a single actuator, thus modification of gait timing must occur during recirculation, so as to not produce inconsistent toe velocities during stance. For RiSE this is even more imperative when climbing a wall because inconsistencies of toe velocities while attached to a climbing surface can cause a robot to lose grip and fall. For this reason, we have developed a variety of prior methods using only gait timing modification during leg recirculation [10, 9] in order to change gaits during locomotion.

This paper focuses upon methods of merging low-level regulation control of gaits, as described above, with high-level task planning, in which hybrid control of various different gait strategies is necessary. We address the problem of producing safe, efficient gait control for underactuated robots via switching policies amongst families of gait limit cycle attractors. We do so by exploiting the algebraic structure of two distinct symbolic decompositions of the limb phase space: the Gait Complex, introduced in Section 2; and the Stance Complex, introduced in Section 3. Our techniques in this paper build upon basic ideas presented in [12], but we introduce methods that are more general and more comprehensive in scope, particular to the application of gait switching. Our specific contributions lie in the introduction of these two cellular decompositions of the phase space that we use to

i. enumerate the allowable gaits of a legged system;
ii. design a mixed planning/control method to navigate amongst them;
iii. execute these transitions in real-time during continuous legged locomotion.

Initial results are presented for a walking hexapod, while future applications include feedback-driven general terrain locomotion for walking, running, and climbing robots, while requiring minimal sensory information and computational power.

2 Hybrid Control Over the Gait Complex

2.1 The Gait Complex, $\mathsf{Gaits}_n[\mathbb{T}]$

In [2], we endow $\mathbb{T}^{n+1}/\mathbb{T} \approx \mathbb{T}^n$ with the structure of a cell complex, denoted $\mathsf{Gaits}_n[\mathbb{T}]$, the disjoint union of its j-skeleta

$$\mathsf{Gaits}_n[\mathbb{T}] = \coprod_{j=0}^{n} \mathsf{Gaits}_n[\mathbb{T}]^j,$$

collections of j-dimensional submanifolds assembled in $\mathsf{Gaits}_n[\mathbb{T}]^j$, with appropriate "gluing" identifications at their boundaries [6]. Although the cardinality of this cell complex must grow combinatorially in the degrees of freedom, n, it is sufficiently regular to enjoy the additional structure of a *Delta Complex* wherein each cell of each of the skeleta is the image of a standard unit simplex whose boundaries are formally associated via a family of "characteristic maps" [6].

We find it useful to index the various cells of the complex, $\mathsf{Gaits}_n[\mathbb{T}]$, by means of equivalence classes of Young Tabloids [16], $\mathcal{T} \in \mathcal{T}_{k+1}^{n+1}$, arrays of (typically) unevenly long strings of integers taken from the set $\{1, \ldots, n+1\}$ with no replacement, each of whose $k+1$ rows denotes a "virtual leg" (a subset of legs that is locked in steady state at the same relative phase for the gait being described), and whose row order corresponds to the cyclic order of virtual legs in the gait. We show formally in [2] that a certain quotient (that is, a complete transversal of left cosets [16] arising from a particular subgroup) of the permutation group $\Sigma_{n+1} \times \Sigma_{k+1}$ is in one-to-one correspondence with the gait complex $\mathsf{Gaits}_n[\mathbb{T}]^k$, but for purposes of this paper it suffices to provide the following intuitive characterization of the equivalence classes as follows. Two tabloids, $\mathcal{T}, \mathcal{T}' \in \mathcal{T}_{k+1}^{n+1}$, index the same cell in the k-skeleton, $\mathsf{Gaits}_n[\mathbb{T}]^k$ if and only if: (i) there is a bijection between their rows (each considered as an unordered collection of integers); and (ii) the bijection is some power of the "full shift", $\zeta \in \Sigma_{k+1} : (1, 2, \ldots, k, k+1) \mapsto (k+1, 1, 2, \ldots, k)$.

In this paper, we make twofold use of the Young Tabloids. First, each Tabloid provides an algorithmic specification of a gait generator over the cell it indexes. We will sketch the nature of this algorithm in Section 2.2 and provide some illustrative examples in Table 6. Second, a computationally simple Tabloid operator, $\partial : \mathcal{T}_{k+1}^{n+1} \rightarrow 2^{\mathcal{T}_k^{n+1}}$ computes the set of tabloids indexing the boundary cells in $\mathsf{Gaits}_{n+1}[\mathbb{T}]^k$ of the cell in $\mathsf{Gaits}_{n+1}[\mathbb{T}]^{k+1}$ indexed by its argument. We will use this operator as the key computational component in the transition planner presented in Section 4. Given length constraints, it does not seem possible in this paper to present any more formal an account of these ideas (which are formally developed in [2]) and we seek rather to provide an intuitive feeling for what the machinery offers through the use of examples and the informal pictures and tables in the Appendix.

2.2 The Gait Fields

While not required for qualification as a Delta Complex, we find in this application the need for a family of "normal" maps $n_{\mathcal{T}} : \mathbb{T}^{n+1} \to \mathbb{T}^{n-k}$ associated with each cell indexed by its tabloid $\mathcal{T} \in \mathcal{T}_{k+1}^{n+1}$ whose Jacobian yields the normal bundle, $Tp_{\mathcal{T}}{}^{\perp}$ defined by the corresponding inclusion map. Specifically, we use them here to build gradient vector fields that "force" the resulting flows toward the designated cell wherein the flow of the desired reference field is known to produce a desired gait. To do so, first observe (as shown formally in [2]) that

$$\nu_m : \mathbb{T}^m \to [0,1] : (r_1, ..., r_m) \mapsto 1 - \frac{1}{m} \sum_{i=1}^{m} \cos \angle r_i \tag{1}$$

is a perfect Morse function with critical points in $\{0, \pi\}^m$ each of which have Morse index specified by number of π entries. It follows that the flow associated with the gradient vector field, $\operatorname{grad} \nu_m$, takes almost all initial conditions in $\mathbb{T}^m$ to the identity, $(e^{2\pi i 0}, \ldots, e^{2\pi i 0})$. Thus, given a tabloid, $\mathcal{T} \in \mathcal{T}_{k+1}^{n+1}$, the Morse function $\nu_{\mathcal{T}} := \nu_{n-k} \circ n_{\mathcal{T}}$ defines a gradient vector field whose flow brings almost every initial condition in $\mathbb{T}^{n+1}$ to the cell in $\mathbb{T}^{n+1}/\mathbb{T}$ that $\mathcal{T}$ indexes. Examples of the normal maps associated with each cell of the three-legged complex, $\mathsf{Gaits}_2[\mathbb{T}]$ are listed in Table 1.

Denote by $R_{BC}^1 : \mathbb{T}^1 \to T\mathbb{T}^1$ the "Buehler Clock" reference generator first introduced in [18] that encodes a one dimensional circulation flow undergoing a phase interval of slow "stance" motion corresponding to the behavior we presume appropriate when a leg is in contact with the ground, followed by a complementary phase interval of fast "recirculation" corresponding to the time interval over which a leg will be lifted off from the ground and returned ready for its next stance phase. This simple rhythm generator can be "pushed forward" to $\mathbb{T}^2$ via the inclusion (5) as $R_{BC}^2 := P_{\boxed{1|2}} \cdot R_{BC}^1 \circ p^{\dagger}{}_{\boxed{1|2}}$. The sum, $F_{PR}^2 = R_{BC}^2 - \operatorname{grad} \nu_{\boxed{1|2}}$, which can be written in angular coordinates (see footnote 3) as

$$F_{PR}^2(x_1, x_2) = R_{BC}^1(x_1) \begin{bmatrix} 1 \\ 1 \end{bmatrix} - \sin(x_1 - x_2) \begin{bmatrix} 1 \\ -1 \end{bmatrix}. \tag{2}$$

induces a flow under which almost every pair of phases is brought to a bipedal "pronk"—a limit cycle characterized by both legs recirculating in phase—a cycle over the cell in $\mathsf{Gaits}_1[\mathbb{T}]$ indexed by $\boxed{1|2} \in \mathcal{T}_1^2$.

In contrast, let us construct the alternating phase bipedal gait generator displaying the archetype of a gait in the "antiphase" cell of $\mathsf{Gaits}_1[\mathbb{T}]$ indexed by $\boxed{\frac{1}{2}} \in \mathcal{T}_1^2$. By conjugation, $R_{AP}^2 := Dh_{TR}^2 \cdot F_{PR}^2 \circ \left(h_{TR}^2\right)^{-1}$, through the translation, $h_{TR}^2 : \mathbb{T}^2 \to \mathbb{T}^2 : (x_1, x_2) \mapsto (x_1, \pi + x_2)$, we define a new vector field

$$R_{AP}^2(x_1, x_2) = R_{BC}^1(x_1) \begin{bmatrix} 1 \\ 1 \end{bmatrix} - \sin(x_1 - x_2 + \pi) \begin{bmatrix} 1 \\ -1 \end{bmatrix}. \tag{3}$$

that shifts the roles of the two invariant submanifolds of the pronking field, F_{PR}^2.

Table 6 provides a detailed listing of the various intermediate fields required to construct two of the most familiar hexapedal gaits: the alternating tripod, R^6_{AP} [18], and the stair climbing gait, R^6_{Stair} [14]. All of the gaits used in the experiments reported here are generated in a similar manner.

3 The Task of Locomotion and the Stance Complex

The Gait Complex, $\mathsf{Gaits}_{n-1}[\mathbb{T}]$, describes all possible gaits for an n-legged robot. Locomotive differences exist, however, amongst the various gaits. We introduce a second cellular decomposition of $\mathbb{T}^n$, the Stance Complex, $\mathsf{Stance}_n[\mathbb{T}]$, to describe the inherent discreteness of legged locomotion and note all possible leg support configurations. We utilize this complex to identify a priori which cells of $\mathsf{Gaits}_{n-1}[\mathbb{T}]$ produce viable statically stable locomotion.

Computation of static stability margin of locomotion can be determined by projecting the mass center onto a support polygon defined by a robot's surface contacts, a computation that can be quite expensive in the presence of complex surface interactions [1]. For a particular contact configuration of limbs, a single cell of $\mathsf{Stance}_n[\mathbb{T}]$, we argue, this stability margin is locally a continuous function of posture, but varies more dramatically (and discretely) when toe contacts are added or removed, other cells of $\mathsf{Stance}_n[\mathbb{T}]$. In the case of underactuated robots, where available postures are limited by low numbers of degrees of freedom, this is particularly true. Even for high degree of freedom system, the workspace of individual limb motions can be quite small when compared to body size, thus expounding the small variation in stability margin within a cell of $\mathsf{Stance}_n[\mathbb{T}]$ compared to dramatic changes when making or breaking contact.

3.1 The Stance Complex

The Gait Complex of Section 2 describes all possible gait timings, noting specific leg phase relationships. Of the immense number of possible gaits, 1082 for a 6-legged robot, not all are locomotively viable, as many may recirculate legs together which produce unstable configurations of the robot's body. $\mathsf{Stance}_n[\mathbb{T}]$ provides us with accurate constraints regarding this aspect of the locomotion task.

Each axis of the n-torus corresponds to the possible gait timings for an individual leg during locomotion, containing both stance and recirculation as discrete regions on the axis. The duty factor of a gait, $\delta \in (0, 2\pi)$, reflects the percentage of stride spent in stance versus recirculation, thus for an individual leg i, if $x_i < \delta$ the leg is considered to be in stance. This demarcation is defined for each axis of the torus, thus producing a complex $\mathsf{Stance}_n[\mathbb{T}]$ of 2^n total cubical cells, as well as intersecting faces and edges. As an example of a cubical member of $\mathsf{Stance}_n[\mathbb{T}]$, consider the cell where $\forall_i x_i < \delta$. This cell corresponds to all legs in stance, while $\forall_i x_i \geq \delta$ is all legs in recirculation.

3.2 Examples: $\mathsf{Stance}_2[\mathbb{T}]$ *and* $\mathsf{Stance}_3[\mathbb{T}]$

If we consider the 2-torus, the space of gait timings for a bipedal robot, there exist four cells shown. One cell on this torus has both legs in stance, two cells have a single leg recirculating, and one cell has both legs recirculating. Assuming a quasi-static locomotory system, it would be dangerous for the robot to use a gait that tries to recirculate both legs at once, thus this last cell should be avoided.

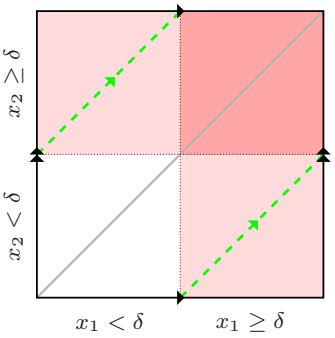

Fig. 1 $\mathsf{Stance}_2[\mathbb{T}]$: Demarcations between stance and recirculation produce 4 unique cells in the Stance Complex. With a stance duty factor of 50% ($\delta = \pi$), there exists only a single gait (dashed line) that does not pass through the cell corresponding to both legs recirculating together (upper right).

Considering a similar system on the 3-torus, depicted as a cube with faces identified in Fig. 2, we demarcate each axis with regions dedicated to stance and recirculation to produce a total of 8 cubical cells in the Stance Complex. Depending upon the exact mechanics of the robot, it may be undesirable to recirculate certain sets of legs together. In the figure we highlight potentially dangerous cells that recirculate 2 or 3 of the legs together at the same time. The cell where all legs are in stance, or only a single leg recirculates, would be considered safe cells.

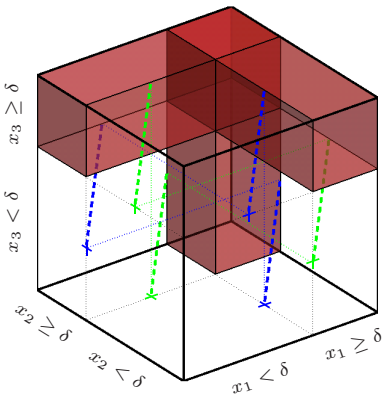

Fig. 2 $\mathsf{Stance}_3[\mathbb{T}]$: A total of 8 unique cubical cells exist in the Stance Complex for the 3-torus. In this figure are highlighted the 4 cells which recirculate 2 or more legs of a 3-legged robot simultaneously. A safe gait, in this scenario, would try to only recirculate a single leg at a time, two such gaits possible when $\delta = \frac{2}{3}2\pi$.

3.3 Static Stability Metric

We utilize $\mathsf{Stance}_n[\mathbb{T}]$ to define in general the global properties of static stability for an n-legged robot. This approach allows us to evaluate gait stability simply by studying the cells through which a given gait passes.

Fig. 3 For basic analysis of static stability, we consider a robot with single actuators per hip, similar to the RHex-style robot shown. With such a model, the stability margin of gaits is computed.

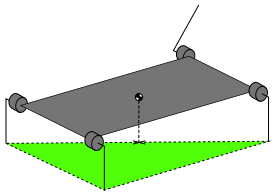

(a) Basic model of rotary joint quadruped

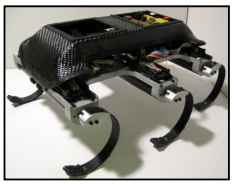

(b) Picture of a RHex-style hexapedal robot

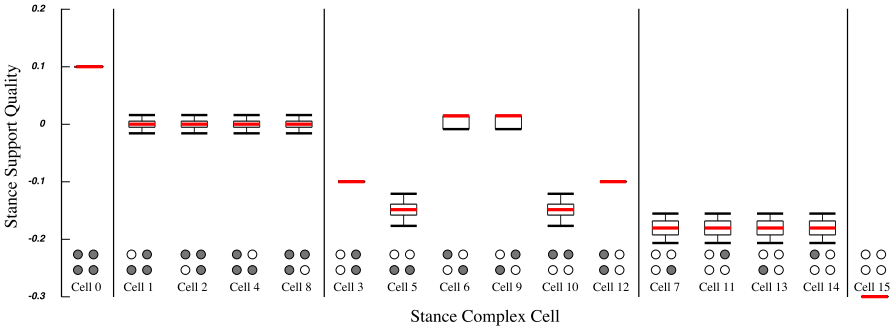

Fig. 4: $\mathsf{Stance}_4[\mathbb{T}]$: There exist 16 cubical cells within $\mathsf{Stance}_4[\mathbb{T}]$, with varying stability values between all. Cells with more legs in stance (represented as shaded circles on simple representations of robot at bottom) have greater stability margins.

Figure 4 shows analysis of the Stance Complex on $\mathbb{T}^4$. Using our simple model of a quadrupedal robot (Fig. 3), each cell is tested for static stability, consisting of a total of $160,000$ tested configurations for the 16 cubical cells, taking into full consideration the entire gait space of $\mathbb{T}^4$. Cells with more legs in stance offer greater static stability. Similarly, certain cells with two legs in stance perform better than others, for instance showing that the cells corresponding to a trot gait, cells 6 and 9, have greater stability than those for pace and bound gaits.

4 Planning and Control Approach

Utilizing both the Gait Complex and Stance Complex, we develop a mixed planning and control approach to automate safe switching between gaits. We intersect cells of $s^{-1}\left(\mathsf{Gaits}_{n-1}[\mathbb{T}]\right)$ with unsafe cells of $\mathsf{Stance}_n[\mathbb{T}]$ in order to prune gait cells that do not produce safe locomotion. A search algorithm is then used to plan routes amongst the remaining cells to generate a sequence of Young Tabloids that are used in a hybrid switching controller that transitions between gaits, while avoiding dangerous, unstable cells of the Stance Complex.

4.1 Transitions on Hasse Diagram of Gaits

The planning component of our hybrid controller relies heavily upon the partial order relation of adjacency by boundary (that we denote by $\succ$) in the Gait Complex. Topologically, it is impossible to pass from one cell to an adjacent neighbor of equal dimension without passing through a "neighbor" on the shared boundary. The very notion of cell adjacency is characterized by this partial order—conveniently captured by the formalism of the *Hasse Diagram* [16]. As different leg combinations incur very different locomotion behaviors (different passages through $\mathsf{Stance}_n[\mathbb{T}]$ in the present problem dealing with static stability) the choice of intermediate cells along the way from one to another gait—i.e., the particular path through the Hasse Diagram—requires a level of methodical scrutiny that we entrust in the present paper to a planner. The strong correspondence between the cellular structure of the Gait Complex, $\mathsf{Gaits}_n[\mathbb{T}]$, and the tabloids, $\mathcal{T}^n$ we use to index it affords our planner a very simple operation over the latter that faithfully represents the boundary operation over the former which we now outline.

Given a tabloid, $T \in \mathcal{T}^{n+1}_{k+1}$, indexing a cell in $\mathsf{Gaits}_n[\mathbb{T}]^k$ there is a very simple operation,

$$\partial : \mathcal{T}^{n+1}_{k+1} \rightarrow 2^{\mathcal{T}^{n+1}_{k}}; \quad 0 \leq k \leq n$$

yielding the tabloids that index all its boundary cells in a manner we merely sketch here (but present rigorously along with a proof of correctness in [2]) as follows. For each pair of contiguous rows of T, collapse the entries into one row comprising the union of the entries of the pair. Compute such a collapsed tabloid for each successive continguous pair of rows, including, finally, the first and the last row, so as to achieve a set of $k+1$ tabloids in $\mathcal{T}^{n+1}_{k}$. Each of these indexes one and only one adjacent (boundary) cell in the $(k-1)$-skeleton, $\mathsf{Gaits}_n[\mathbb{T}]^{k-1}$. Hopefully, it is intuitively clear that the "tabular inverse" of this operation,

$$\partial^{-1} : \mathcal{T}^{n+1}_{k} \rightarrow 2^{\mathcal{T}^{n+1}_{k+1}}, \quad 0 \leq k \leq n$$

yields the one-row-longer tabloids that index the cells that share a boundary component indexed by the argument. For example the partial order adjacency relation at the quadrupedal "half-bound" gait (for example reported in [8]) is computed as

$$\left\{\begin{smallmatrix}\boxed{1}\\\boxed{2}\\\boxed{3}\\\boxed{4}\end{smallmatrix}, \begin{smallmatrix}\boxed{1}\\\boxed{2}\\\boxed{4}\\\boxed{3}\end{smallmatrix}\right\} = \partial^{-1}\left\{\begin{smallmatrix}\boxed{1}\\\boxed{2}\\\boxed{3}\boxed{4}\end{smallmatrix}\right\} \succ \left\{\begin{smallmatrix}\boxed{1}\\\boxed{2}\\\boxed{3}\boxed{4}\end{smallmatrix}\right\} \succ \partial\left\{\begin{smallmatrix}\boxed{1}\\\boxed{2}\\\boxed{3}\boxed{4}\end{smallmatrix}\right\} = \left\{\begin{smallmatrix}\boxed{1}\boxed{3}\boxed{4}\\\boxed{2}\end{smallmatrix}, \begin{smallmatrix}\boxed{1}\\\boxed{2}\boxed{3}\boxed{4}\end{smallmatrix}, \begin{smallmatrix}\boxed{1}\boxed{2}\\\boxed{3}\boxed{4}\end{smallmatrix}\right\}$$

Considering legs in recirculation, this definition of adjacency makes intuitive sense: when multiple legs enter recirculation together, as legs within the same row of a tabloid would, it is possible for one leg to speed up while another slows, thus splitting the row apart as the current gait cell changes. Conversely, legs entering recirculation may wait indefinitely for other legs—so long as the robot remains statically stable—such that they synchronize, merging rows of a tabloid.

Using this definition of adjacency between tabloids, and starting from the initial "pronk" tabloid on $\mathbb{T}^6$, $\boxed{1}\boxed{2}\boxed{3}\boxed{4}\boxed{5}\boxed{6}$, we build an adjacency matrix amongst all 1082 cells of $\mathsf{Gaits}_5[\mathbb{T}]$, shown in Fig. 5a. This matrix is block adjacent, since a given tabloid may only be adjacent to cells with either one less or one more length in rows. If we extend our definition of adjacency to allow multiple *sequential* rows to be compressed together (or a single row split into more than rows)—a reflection that more than two groups of legs can split or join in a given operation (or, more topologically, that we will allow immediate passage to boundaries of boundaries of cells in the gait complex)—this expands the definition of the Hasse Diagram to include other adjacencies, shown in Fig. 5b.

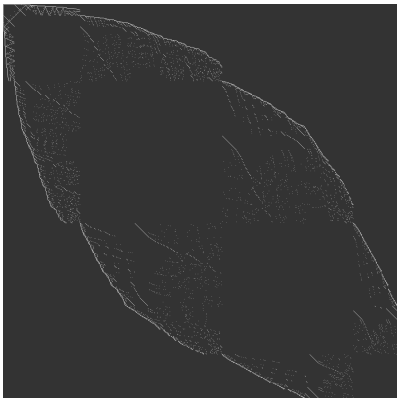

(a) Hasse Diagram of Young Tabloids

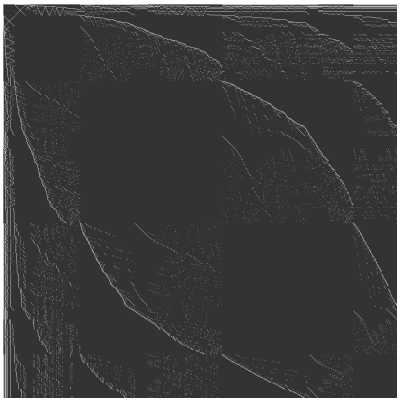

(b) Hasse Diagram including multi-dimensional adjacency

Fig. 5: Hasse Diagrams over the set of Young Tabloids. A 1082×1082 matrix represents the graph of gait cells, white dots representing adjacency. Cells are in order of increasing dimensionality, block-wise groupings shown here, prior to filtering based upon the Stance Complex.

Lastly, before applying a discrete planner over this set of gait cells, we prune based upon static stability. In our basic implementation of the Stance Complex, we limit ourselves to cells that do not recirculate either ipsilateral nor contralateral legs (excluding the middle pair) together, thus only allowing 18 out of the 64 cells of $\mathsf{Stance}_n[\mathbb{T}]$. This conservative restriction on the Stance Complex, when intersected with the Gait Complex, reduces allowable gait cells to only 477 of the original 1082,

however all 477 are statically stable gaits. Another result of the conservative estimate of gait stability is the existence of disconnected clusters of gaits in the Gait Complex. Of the 477 gaits, 301 exist in one large cluster (including the most commonly accessed legged gaits for $N = 6$) with another two symmetric clusters of 87 gaits, while each of the two circular crawls is likewise disconnected from all other gaits. By our estimation of static stability, it is impossible to reach one cluster from another, due to our constraints on ipsilateral and contralateral legs.

4.2 Planning Gait Complex Switching

We consider the problem of an underactuated robot, where freedom to control leg phasing only occurs during recirculation. To discretely plan over this set of operations, we utilize an A* planner that computes cost, in terms of total transition time, between arbitrary cells of the Gait Complex.

The cost of an individual transition between two cells depends upon the initial phase of the first gait. Given that legs must recirculate together to switch, we sum the wait time until legs begin recirculation with total time of recirculation to get actual cost. An admissible heuristic in this case is cost of 1.0, as adjacent cell transitions cannot take more than one stride.

4.3 Controller Activation

Our controllers take a given sequence of tabloids, as output by the A* planner, and construct individual reference field controllers, following from the examples in Section 2.2. Several additional controller modifications are as follows.

Foremost, active control of leg phase occurs only during recirculation. We assume legs in stance to be "rigidly" attached to the surface, particularly relevant when considering climbing robots where inappropriate torquing of individual feet may cause them to lose grasp. In this way, the gradient field simply zeros any action along axes for legs currently in stance.

The duty factor of the system is also modified when the robot approaches new gaits. A virtual biped gait, such as the alternating tripod, will use a gait with 50% duty factor when close in phase space. A simple controller that provides an algebraic relationship between duty factor and phase is detailed in [7].

Lastly, in our definition of the reference field controllers, we leave freedom in the choice of the exact structure of an individual tableaux. [1]

$$t(\begin{smallmatrix}\boxed{1}\boxed{2}\\ \boxed{3}\boxed{4}\end{smallmatrix}) = \{\begin{smallmatrix}\boxed{1}\boxed{2}\\ \boxed{3}\boxed{4}\end{smallmatrix}, \begin{smallmatrix}\boxed{2}\boxed{1}\\ \boxed{3}\boxed{4}\end{smallmatrix}, \begin{smallmatrix}\boxed{1}\boxed{2}\\ \boxed{4}\boxed{3}\end{smallmatrix}, \begin{smallmatrix}\boxed{2}\boxed{1}\\ \boxed{4}\boxed{3}\end{smallmatrix}\}$$

Each tableaux describes the same system, consisting of the same limit cycle gait, with different enumerations of legs within the rows of the tableux. The distinction

[1] Following the terminology of [16], a *tabloid* is the equivalence class of all numerically filled-in diagrams whose rows are identical, disregarding the order of the integer entries of each row.

between individual tableaux, however, affects the construction of the related reference field controllers, as the first element of each row is chosen as *leader* (formally specified by the choice of left inverse as exemplified by $p_{\boxed{1}\boxed{2}}$ in equation (5)). To effect a rational choice of "leader" in any new instantiation of a gait, we consider all identified tableaux of a specific tabloid T, and make use of the one whose potential function has the lowest value.

$$\underset{\mathsf{T}' \in t(\mathsf{T})}{\operatorname{argmin}} \; \nu_{\mathsf{T}'}(r)$$

By selecting the minimum cost potential function from which to generate our reference field, we achieve an online adjustment of the transient behaviors of the system such that it follows near-minimum distance paths between gaits, without introducing local minima (as each possible x has the same stable critical point and our system always decreases in potential). For an alternating tripod gait, this operation includes a total of 36 function evaluations in order to choose an ordering.

5 Experimental Results

Using a hexapedal robot platform, we have implemented our gait transition method and shown its efficacy in producing near arbitrary transitions between safe gaits while preventing loss of static stability. We discuss examples of such transitions, compare with a naïve coupled oscillator approach, and project directions in which this research will enable new behaviors for both walking and climbing legged robots.

5.1 Gait Switching

Our new gait switching methods attempt to rectify deficiencies in our prior approaches. For the domain of climbing robots, we have constructed hand-designed transitions between gaits [10], but these transitions were not easily generated nor guaranteed. Further work produced control laws that converged to desired gaits [7], but was limited to a small number of gaits with no choice of which exact gait to converge. The methods described here attempt to automate the generation of transitions, allow transitions between arbitrary pairs of gaits, while preventing static instability.

Fig. 6 shows the transition from a crawl gait to the alternating tripod gait.The top of the figure shows the sequence of tabloids that the planner has determined to converge the fastest. The bottom plot shows roll, pitch, and yaw angles, relatively stable while undergoing a transition of gait.

Fig. 7 shows two different attempts to produce a non-trivial gait transition. The first uses the tabloid-derived control law to simply converge to the desired gait, however it has the undesireable results of poorly designed paths of convergence, following from a basic coupled oscillator approach [12]. The second uses a sequence of planned intermediary gaits to produce a transition that retains static stability.

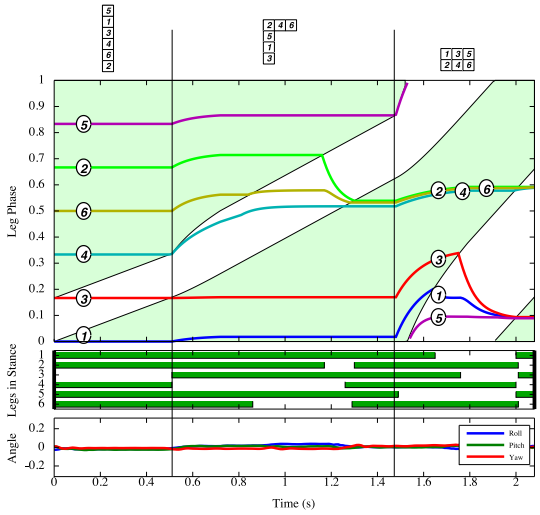

Fig. 6 A sequenced transition of Young Tabloids between gaits. At each switch time, the controller changes, converging to the next gait. End result is a transition behavior that avoids static instabilities. Each line is a "phase offset" of a given leg [**?**], with green regions indicating stance. Phase control occurs during recirculation while adjustment of duty factor (ratio of green to white) takes place as the system reaches desired gaits.

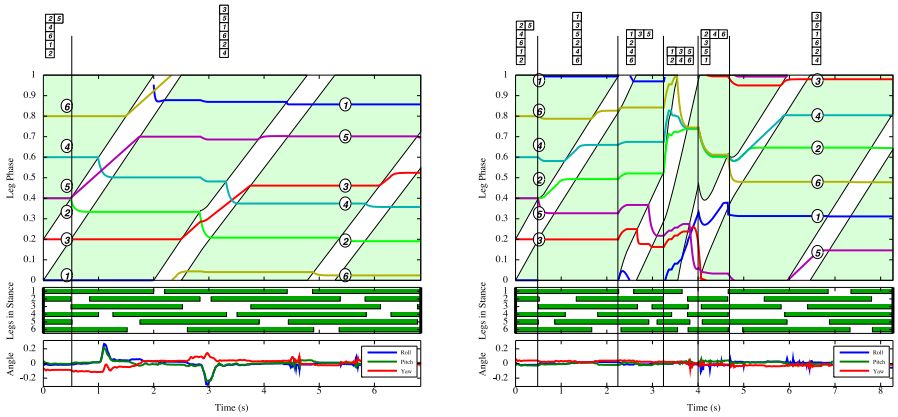

(a) Direct Controller Transition

(b) Planned Sequence of Controllers

Fig. 7: Two transitions between gaits. The planned sequence (right) prevents loss of static stability, while the direct approach (left) loses static instability, as measured by pitch-roll-yaw angles from a Vicon system.

As can be seen in the plots, the unplanned version recirculates too many legs together, loses static stability, and pitches, rolls, and yaws during the transition. The planned version remains relatively level throughout the entire transition. Inconvenient and disruptive during a level ground walk, such perturbations would be catastrophic in a climbing setting, or even, most likely, in a high performance dynamical level ground setting.

6 Conclusions and Future Work

We have introduced a combined planning and control method that uses both discrete and continuous representations to plan and execute transitions amongst gaits implemented on an underactuated legged robot. Introduction of both the Gait Complex, a structure that characterizes all the possible one-cycles achievable with an n-legged machine, as well as the Stance Complex, classifying the ground contact status of all legs, brings about a greater understanding of the space of gaits, and points the way to global approaches for gait control.

In these preliminary experimental results, it seems possible that naïve transitions using gaits that simply avoid bad cells of the Stance Complex may perform just as well as the planner's sophisticated use of cell adjacency. Furthermore, the situation is of course a good deal more complex than we allow in this first paper on these cellular decompositions. For example, the present gait reference fields (Sec. 2) yield steady state limit cycles whose paths maintain rigid phase relationship amongst legs. There is no reason not to consider more general gaits whose orbits may wind about the torus in different ways in order to avoid bad cells of the Stance Complex. [2]

We are currently studying methods of extending our level-ground transitions to domains in which the terrain varies, such as climbing over rubble-like obstacles or transitions between level-ground locomotion and vertical climbing, in which we expect different sets of viable gaits to be available to us. In both of these cases, studying how body geometry and contact mechanics affect the allowable cells of the Gait and Stance Complexes is part of our future work.

Acknowledgements This work was supported in part by the ONR HUNT project, the DARPA SToMP project, and an Intelligence Community Postdoctoral Fellowship held by the first author.

Appendix A: The Gait Complex and its Defining Inclusions

The gait complex $\mathsf{Gaits}_n[\mathbb{T}]$ is a cellular decomposition of $\mathbb{T}^n$ built upon the image of $\mathbb{T}^{n+1}$ under the "shearing map" [3],

$$s^{n+1} : \mathbb{T}^{n+1} \to \mathbb{T}^n : (r_1, \ldots, r_n, r_{n+1}) \mapsto (r_1 r_{n+1}^{-1}, \ldots, r_n r_{n+1}^{-1}). \qquad (4)$$

The cells of $\mathsf{Gaits}_n[\mathbb{T}]$ arise by "shearing" down all of the "diagonal" subspaces of $\mathbb{T}^{n+1}$—that is, all of those orbits wherein some subset of entries maintain the identical phase—and thus represent via a single n-tuple, an "orbit" of $(n+1)$-tuples that circulate while maintaining the same relative phase. [3]

[2] For an example of a more complicated family of reference gait generators capable of producing such "winding" limit cycles, consider the example in Fig. 3 of [20].

[3] We will shift back and forth as a matter of convenience between representing phase as an "angle" x, or as a point on the unit circle in the complex plane, $r = e^{2\pi i x}$, where e is the standard exponential map.

For example, the bipedal steady state gaits may be coarsely distinguished by whether or not the legs are held in the same phase ("pronking") during circulation through periodic stride. Following the account at the beginning of Section 2.2, we use the Young Tabloid $\mathcal{T} = \boxed{1|2} \in \mathcal{T}_1^2$ to index the bipedal "Pronk" by defining a parametrization of the appropriate diagonal,

$$p_{\boxed{1|2}} : \mathbb{T}^1 \to \mathbb{T}^2 : r \mapsto (r, r); P_{\boxed{1|2}} := Dp_{\boxed{1|2}} = \begin{bmatrix} 1 \\ 1 \end{bmatrix}; \quad p^{\dagger}{}_{\boxed{1|2}}(r_1, r_2) := r_1, \tag{5}$$

(that we display along with its Jacobian matrix, $P_{\boxed{1|2}}$, and a choice of left inverse , $p^{\dagger}{}_{\boxed{1|2}}$, made apparent in the discussion of Section 2.2) which is then "sheared down" to get the representative cell, $\mathsf{Gaits}_1[\mathbb{T}]^0 = \left\{ s^2 \circ p_{\boxed{1|2}}(\mathbb{T}^1) \right\}$—in this case, the single"vertex" $s^2 \circ p_{\boxed{1|2}}(r) = e^{2\pi i 0}$. In contrast, if the legs are out of phase in steady state, then we locate the gait in the sheared image of the identity map of the two-torus to get $\mathsf{Gaits}_1[\mathbb{T}]^1 = \left\{ s^2 \circ p_{\mathcal{T}}(\mathbb{T}^2) \right\}$ for $\mathcal{T} = \boxed{\frac{1}{2}} \in \mathcal{T}_2^2$, which evaluates to the entire "circle" $s^2 \circ p_{\mathcal{T}}(r_1, r_2) = e(2\pi i(x_1 - x_2))$. The Delta Complex formalism [6] requires these inclusions be made from the domain of a simplex,

$$\begin{aligned} \Delta[m] := \{(x_1, x_1 + x_2, \ldots, x_1 + \ldots + x_m) \in [0,1]^m : \\ 0 \leq x_1 + \ldots + x_j \leq 1, j = 1, \ldots m\} \end{aligned}$$

and given a Young Tabloid, $\mathcal{T} \in \mathcal{T}_{k+1}^{n+1}$ with toral inclusion, $p_{\mathcal{T}} : \mathbb{T}^{k+1} \to \mathbb{T}^{n+1}$, the associated "characteristic function" is $\tilde{p}_{\mathcal{T}} := p_{\mathcal{T}} \circ exp^{k+1}$ where $exp^m : \Delta[m] \to \mathbb{T}^m : (x_1, \ldots, x_m) \mapsto (e^{2\pi i x_1}, \ldots, e^{2\pi i x_m})$. Continuing along this specific example, for $m = n + 1 = 2$, the Delta Complex formalism now re-assembles these two sets—the zero-skeleton, $\mathsf{Gaits}_1[\mathbb{T}]^0$, and the one-skeleton $\mathsf{Gaits}_1[\mathbb{T}]^1$—into the cell complex, $\mathsf{Gaits}_1[\mathbb{T}] = \mathsf{Gaits}_1[\mathbb{T}]^0 \coprod \mathsf{Gaits}_1[\mathbb{T}]^1$ by identifying their shared point $e^{2\pi 0}$ via the characteristic maps as detailed in [2]. The corresponding generalization of this construction to the 3-legged gait complex is listed in Table 1 and depicted in Figure 8 which also provides a view of the 4-legged gait complex.

References

1. Bretl, T., Lall, S.: Testing static equilibrium for legged robots. IEEE Transactions on Robotics **24**(4), 794–807 (2008)
2. Cohen, F., Koditschek, D.E.: Hybrid control over the coordination complex. (in preparation) (2009)
3. Cohen, F.R.: On Configuration Spaces. (in preparation) (2008)
4. Farley, C., Taylor, C.: A mechanical trigger for the trot-gallop transition in horses. Science **253**, 306–308 (1991)
5. Griffin, T., Kram, R., Wickler, S., Hoyt, D.: Biomechanical and energetic determinants of the walk-trot transition in horses. Journal of Experimental Biology **207**, 4215–4223 (2004)
6. Hatcher, A.: Algebraic topology. Cambridge Univ. Press (2002)
7. Haynes, G.C.: Gait regulation control techniques for robust legged locomotion. Ph.D. thesis, Robotics Institute, Carnegie Mellon University, Pittsburgh, PA (2008)

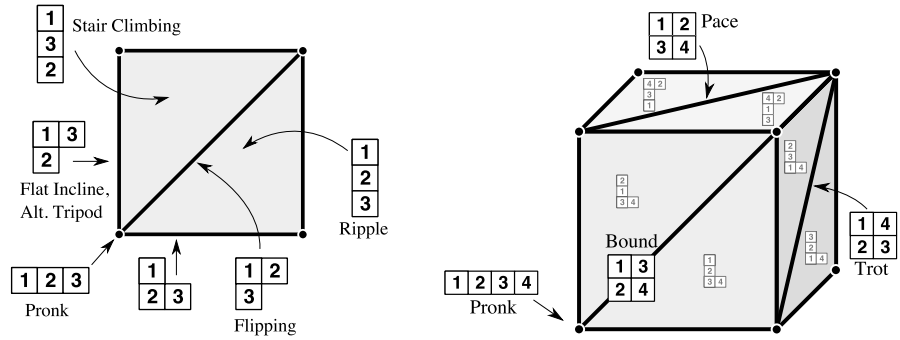

(a) $\mathsf{Gaits}_2[\mathbb{T}]$ from $s^3 \circ p_T : \mathbb{T}^3 \to \mathbb{T}^2$ (b) $\mathsf{Gaits}_3[\mathbb{T}]$ from $s^4 \circ p_T : \mathbb{T}^4 \to \mathbb{T}^3$

Fig. 8: An exhaustive view of the cells of the "three-legged" gait complex (left) and a typical view of the "four-legged" gait complex (right) annotated by their associated Young Tabloids, T, and examples of some of the gaits they represent.

Tabloid $T \in \mathcal{T}^3_{k+1}$	InclusionMaps $\Delta[k+1] \xrightarrow{\tilde{p}_T} \mathbb{T}^3 \xrightarrow{s^3} \mathbb{T}^2$	NormalMap $n_T(r_1, r_2, r_3)$	Gait Name
1 2 3	$(x) \mapsto (e^{2\pi i x}, e^{2\pi i x}) \mapsto (e^{2\pi i 0})$	$(r_1 r_3^{-1}, r_2 r_3^{-1})$	Pronk
1 2 3	$(x_1, x_1 + x_2) \mapsto (e^{2\pi i x_1}, e^{2\pi i x_1}, e^{2\pi i (x_1 + x_2)}) \mapsto (e^{-2\pi i x_2}, e^{-2\pi i x_2})$	$r_1 r_2^{-1}$	Reverse Flip
1 3 2	$(x_1, x_1 + x_2) \mapsto (e^{2\pi i x_1}, e^{2\pi i (x_1 + x_2)}, e^{2\pi i x_1}) \mapsto (e^{2\pi i 0}, e^{2\pi i x_2})$	$r_1 r_3^{-1}$	Incline
2 3 1	$(x_1, x_1 + x_2) \mapsto (e^{2\pi i (x_1 + x_2)}, e^{2\pi i x_1}, e^{2\pi i x_1}) \mapsto (e^{2\pi i x_2}, e^{2\pi i 0})$	$r_2 r_3^{-1}$	Flip
1 2 3	$(x_1, x_1 + x_2, x_1 + x_2 + x_3) \mapsto$ $(e^{2\pi i x_1}, e^{2\pi i (x_1 + x_2)}, e^{2\pi i (x_1 + x_2 + x_3)}) \mapsto (e^{-2\pi i (x_2 + x_3)}, e^{-2\pi i x_3})$	$\emptyset$	Ripple
1 3 2	$(x_1, x_1 + x_2, x_1 + x_2 + x_3) \mapsto$ $(e^{2\pi i x_1}, e^{2\pi i (x_1 + x_2 + x_3)}, e^{2\pi i (x_1 + x_2)}) \mapsto (e^{-2\pi i x_2}, e^{2\pi i x_3})$	$\emptyset$	StairClimbing

Table 1: The Gait Complex $\mathsf{Gaits}_2[\mathbb{T}]$

Gait	Field	Formula	Change of Coordinates
Bipedal Pronk [18]	R^2_{PR}	$P_{\boxed{1}\boxed{2}} \cdot R^1_{BC} \circ {p^\dagger}_{\boxed{1}\boxed{2}} - \operatorname{grad} \nu_{\boxed{1}\boxed{2}}$	$\emptyset$
Alternating Phase Biped [18]	R^2_{AP}	$Dh^2_{TR} \cdot R^2_{PR} \circ \left(h^2_{TR}\right)^{-1}$	$(x_1, x_2) \mapsto (x_1, x_2 + \pi)$
Three-Legged Pronk [13]	R^3_{PR}	$P_{\boxed{1}\boxed{2}\boxed{3}} \cdot R^1_{BC} \circ {p^\dagger}_{\boxed{1}\boxed{2}\boxed{3}} - \operatorname{grad} \nu_{\boxed{1}\boxed{2}\boxed{3}}$	$\emptyset$
Three-Legged Crawl [14]	R^3_{CR}	$Dh^3_{TR^+} \cdot R^3_{PR} \circ \left(h^3_{TR^+}\right)^{-1}$	$(x_1, x_2, x_3) \mapsto (x_1, x_2 - \frac{4\pi}{3}, x_3 - \frac{2\pi}{3})$
Hexapedal Alternating Tripod [18]	R^6_{AP}	$P_{\begin{smallmatrix}\boxed{1}\boxed{4}\boxed{5}\\ \boxed{2}\boxed{3}\boxed{6}\end{smallmatrix}} \cdot R^2_{AP} \circ {p^\dagger}_{\begin{smallmatrix}\boxed{1}\boxed{4}\boxed{5}\\ \boxed{2}\boxed{3}\boxed{6}\end{smallmatrix}} - \operatorname{grad} \nu_{\begin{smallmatrix}\boxed{1}\boxed{4}\boxed{5}\\ \boxed{2}\boxed{3}\boxed{6}\end{smallmatrix}}$	$\emptyset$
Hexapedal Stair Gait [13]	R^6_{Stair}	$P_{\begin{smallmatrix}\boxed{1}\boxed{2}\\ \boxed{3}\boxed{4}\\ \boxed{5}\boxed{6}\end{smallmatrix}} \cdot R^3_{CR} \circ {p^\dagger}_{\begin{smallmatrix}\boxed{1}\boxed{2}\\ \boxed{3}\boxed{4}\\ \boxed{5}\boxed{6}\end{smallmatrix}} - \operatorname{grad} \nu_{\begin{smallmatrix}\boxed{1}\boxed{2}\\ \boxed{3}\boxed{4}\\ \boxed{5}\boxed{6}\end{smallmatrix}}$	$\emptyset$

Table 2: Gait Fields over Limb Phase Coordinates.

8. Haynes, G.C., Khripin, A., Lynch, G., Amory, J., Saunders, A., Rizzi, A.A., Koditschek, D.E.: Rapid pole climbing with a quadrupedal robot. In: Proc. IEEE International Conference on Robotics and Automation (2009)
9. Haynes, G.C., Rizzi, A.A.: Gait regulation and feedback on a robotic climbing hexapod. In: Proceedings of Robotics: Science and Systems. Philadelphia, USA (2006)
10. Haynes, G.C., Rizzi, A.A.: Gaits and gait transitions for legged robots. pp. 1117–22. Orlando, FL, USA (2006)
11. Hildebrand, M.: Symmetrical gaits of horses. Science **150**, 701–708 (1965)
12. Klavins, E., Koditschek, D.: Phase regulation of decentralized cyclic robotic systems. International Journal of Robotics Research **21**(3) (2002)
13. McMordie, D., Buehler: Towards pronking with a hexapod robot. In: Proc. 4th Intl. Conf. on Climbing and Walking Robots, pp. 659–666. Storming Media, Karlsruhe, Germany (2001)
14. Moore, E.Z., Campbell, D., Grimminger, F., Buehler, M.: Reliable stair climbing in the simple hexapod'rhex'. In: Robotics and Automation, 2002. Proceedings. ICRA'02. IEEE International Conference on, vol. 3 (2002)
15. Muybridge, E.: Animals in Motion. Dover Publications, New York (1899)
16. Sagan, B.: The Symmetric Group: Representations, Combinatorial Algorithms and Symmetric Functions. Wadsworth and Brooks/Cole, Mathematics Series (1991)
17. Saranli, U., Buehler, M., Koditschek, D.E.: RHex: A Simple and Highly Mobile Hexapod Robot. The International Journal of Robotics Research **20**(7), 616–631 (2001). DOI 10.1177/02783640122067570
18. Saranli, U., Buehler, M., Koditschek, D.E.: Rhex: A simple and highly mobile hexapod robot. The International Journal of Robotics Research **20**, 616 (2001)
19. Spenko, M.A., Haynes, G.C., Saunders, A., Rizzi, A.A., Cutkosky, M., Full, R.J., Koditschek, D.E.: Biologically inspired climbing with a hexapedal robot. Journal of Field Robotics **25**(4-5) (2008)
20. Weingarten, J.D., Groff, R.E., Koditschek, D.E.: A framework for the coordination of legged robot gaits. In: Robotics, Automation and Mechatronics, 2004 IEEE Conference on (2004)
21. Wickler, S., Hoyt, D., Cogger, E., , Myers, G.: The energetics of the trot-gallop transition. Journal of Experimental Biology **206**, 1557–1564 (2003)
22. Wilson, D.M.: Insect walking. Annual Review of Entomology **11**, 103 – 122 (1966)